Communication

Not peer-reviewed version

Investigation of Microstructure and Mechanical Properties of Tungsten Irradiated by Helium Plasma

Aidar Kengesbekov *, Bauyrzhan Rakhadilov, Zarina Satbaeva

Posted Date: 20 November 2023

doi: 10.20944/preprints202311.1205.v1

Keywords: plasma; linear plasma devices; plasma-surface interactions; vacuum; KAZ-PSI doi:10.20944/preprints202311.1205.v1

Communication

Investigation of Microstructure and Mechanical Properties of Tungsten Irradiated by Helium Plasma

Aidar Kengesbekov [1,*] Bauyrzhan Rakhadilov [2] and Zarina Satbaeva [2]

[1] PlasmaScience LLP, Ust-Kamenogorsk 070000, Kazakhstan
[2] Institute of Composite Materials Ust Kamenogorsk 070000, Kazakhstan; rakhadilovb@mail.ru (B.R.); satbaeva.z@mail.ru (Z.S.)
* Correspondence: aidar.94.01@mail.ru; Tel.: +7-777-245-2066.

Abstract: The paper presents the results of the study of tungsten surface structure modification under helium plasma irradiation. It is revealed that during irradiation of samples, surface modification in the form of relief development as a result of irradiation is observed. X-ray phase analysis showed that no new phases of the W system were found after irradiation, only an increase in the intensity of diffraction lines was observed. There are significant differences in the microstructure of tungsten depending on the temperature of helium plasma irradiation in the above range. It is assumed that the cause of defects is the extremely low solubility of helium in tungsten. Metallographic analysis has shown that at irradiation of tungsten samples in regime 5 and 6 the degree of relief development is not high in comparison with the tungsten sample irradiated in regime 4. The greatest increase in roughness of the sample irradiated in regime 5 was determined, which is associated with the formation of small cracks, blisters and pores in the surface layer. At the same time, in the samples irradiated in regime 6, the surface of which is characterized by chaotically located protrusions and depressions of various shapes, the roughness parameter Ra was 0.0603 μm. It was found that at temperature regimes T = 1200 °C and T = 1500 °C the microhardness of tungsten increases by 11% and 10% respectively.

Keywords: plasma, linear plasma devices, plasma-surface interactions, vacuum, KAZ-PSI

1. Introduction

Tungsten stands out as the primary material choice for plasma-exposed surfaces in future nuclear fusion power devices because it offers a unique blend of characteristics, including a low sputtering rate, minimal activation during transmutation, and excellent thermal conductivity [1]. When employed in a plasma-facing role, it will endure some of the most extreme conditions encountered by engineering materials, including surface temperatures exceeding 1000°C, damage levels reaching up to 50 dpa/yr from 14.1 MeV neutrons, compositional changes of up to 5 at. % due to transmutation over the operational lifespan, and the direct implantation of helium from the plasma [2]. Deterioration of tungsten under these circumstances will constrain the component's longevity and negatively impact the efficiency of the fusion plasma, as sputtered tungsten atoms and dust ingress. The combined effects of damage caused by neutrons and helium, originating from both transmutation and plasma injection, will induce substantial alterations in tungsten's mechanical properties [3,4]. A crucial aspect is comprehending the underlying mechanisms governing these effects, as it is essential for modeling the failure mechanisms of plasma-facing tungsten. Previous studies have predominantly focused on elucidating the mechanisms leading to the creation of bubbles, voids, and "nano-fuzz" in tungsten due to helium exposure [5].

Chen et al. [6] conducted a study in which they subjected PM2000 ODS steel to simultaneous and sequential implantations of Fe+ ions and He+ ions. These implantations were carried out on the as-received material and on material cold-rolled to 30% and 70% reduction in thickness, resulting in damage levels of 31 dpa and 18 appm/dpa of helium. They observed an increase in hardness, measuring 1.15 GPa for the as-received material, 0.23 GPa for the 30% rolled material, and 0.2 GPa for the 70% rolled material. In the case of the two rolled materials, the hardness increases fell within one standard deviation of the unirradiated hardness. This implies that the rolling process generates

Preprints (www.preprints.org) | NOT PEER-REVIEWED | Posted: 20 November 2023 doi:10.20944/preprints202311.1205.v1

defects that act as traps for helium and displacement damage, thereby diminishing their hardening impact.

Kogler et al. [7] also conducted Fe/He implantations on PM2000, both in its as-received state and after heat treatment. They performed both sequential and simultaneous implantations, resulting in damage levels of 52 dpa and 20.7 appm He/dpa. In the as-received materials, simultaneous implantation led to a substantially higher hardening effect (1 GPa) compared to sequential implantation, while in the heat-treated case, the material implanted simultaneously with Fe and He exhibited only a 0.3 GPa increase in hardness compared to the sequentially implanted material.

Hunn et al. [8] carried out helium implantation on 316LN stainless steel, using 360 keV helium ions to reach a level of 332 appm. This resulted in significant hardness increases, up to 2 GPa, in the area with the highest damage, associated with the formation of helium bubbles. In contrast, Fe+ ion implantation at similar damage levels produced hardness increases that were 50% lower.

These studies have highlighted that helium implantation can lead to a more pronounced hardening effect than self-ion implantation, and there are variations in hardness between sequential and simultaneous implantations in ferritic alloys. However, while there have been numerous investigations into the mechanical properties of both neutron- and self-ion-implanted tungsten alloys, with substantial hardness increases of up to 3 GPa observed, there has been no prior research on the influence of helium implantation on tungsten's mechanical properties [9-11].

In this work, we investigate the effect of He-plasma exposure on W samples. In this regard, a new laboratory linear plasma unit, KAZ-PSI, was designed and built to test candidate divertor materials and to perform plasma-surface interaction studies.

The purpose of this work is to investigate the effect of helium plasma irradiation on the structural-phase state and mechanical properties of tungsten.

2. Materials and Methods

2.1. Parameters of Plasma Unit

The KAZ-PSI plasma facility [12], built at PlasmaScience LLP in 2019, Fig.1., is designed for plasma testing of refractory metals and materials created by electron beam irradiation. The setup is a linear system with a magnetic plasma confinement scheme.

Parameters of the plasma unit:

- longitudinal magnetic field on the axis – up to 0.3 T;
- internal diameter of the discharge chamber – 0,15 m;
- length of the discharge chamber - 1 m; the chamber is equipped with a water-cooling circuit, which provides a stationary discharge mode;
- plasma discharge current – up to 1 A;
- plasma density – 1018 cm-3;
- electron temperature – up to 20 eV;
- negative displacement at the cathode relative to the grounded anode – 0-2 kV
- injected electron beam power – up to 10 kW

Preprints (www.preprints.org) | NOT PEER-REVIEWED | Posted: 20 November 2023 doi:10.20944/preprints202311.1205.v1

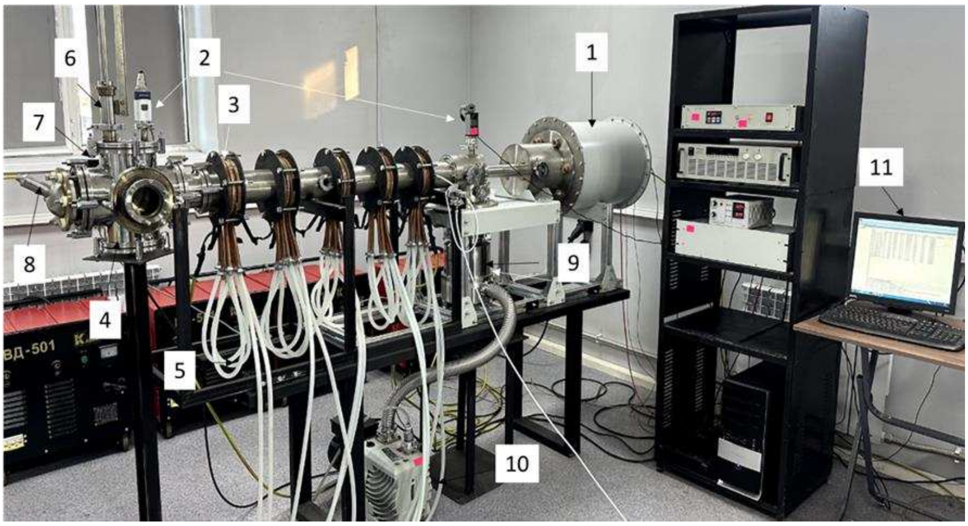

Figure 1. General view of the linear plasma unit KAZ-PSI.

The main components of the small-sized linear stimulator are - 1) electron gun, 2) vacuum sensor, 3) system of electromagnetic coils, 4) interaction chamber, 5) cooling target, 6) Langmuir probe, 7) negative potential, 8) residual gas analyzer, 9) turbomolecular pump, 10) forevacuum pump, 11) personal computer to control the KAZ-PSI unit. The general principle of operation of the KAZ-PSI unit consists of the following principles: the electron gun forms an electron beam of axially symmetrical character, the gun cathode is heated by electron bombardment from the heater filament, which contributes to the adjustment of the gun power. The vacuum drop between the gun and the discharge chamber is realized by autonomous pumping of the gun. The plasma cord is formed in the discharge chamber by the interaction of the electron beam with the working gas - helium. In the discharge chamber with the help of coil systems, which creates a longitudinal magnetic field, the focusing of electron and plasma beams is realized. By changing the value of electric current flowing through electromagnetic coils, it is possible to manipulate the value of magnetic field strength in the plasma-beam discharge chamber, thereby controlling the beam diameter. The plasma discharge hits a sample of the material to be tested, which is placed on a target device in the interaction chamber.

This facility is planned to test materials under the complex high-energy effects of a stationary hot plasma. Such studies will advance the understanding of the physics of interaction of hot plasma with materials such as tungsten, molybdenum, steel, ITER wall and diverter materials, and others. The relevance of research work on this facility is related to the observation of increased erosion of tungsten in co-modern fusion facilities, which needs to be investigated in full-scale experiments to establish the physical mechanisms of erosion. Therefore, the problem of improving the performance characteristics of materials remains one of the important tasks of materials science and in the field of thermonuclear fusion.

2.2. Experimental procedure

In this work, the interaction of helium plasma with tungsten was studied using the developed KAZ-PSI unit. Tungsten samples of 99.95% purity in the form of a cylinder with a diameter of 10 mm and a height of 5 mm were ground and polished. The samples were irradiated with a plasma beam in helium medium. The parameters of the experiments are shown in Table 1.

Table 1. Parameters of tungsten irradiation with helium plasma.

No.	Irradiation time, h	Helium pressure, ×10^{-4} Torr	Power of the electronic gun, kW	Negative potential on the target, V	Target temperature, °C	Ion fluence, m^2
1	0.5	1.2±0.05	0.42	1500	900±10	2.4 ×10^{25}
2	0.5		0.57		1200±10	2.4 ×10^{25}
3	0.5		0.71		1500±10	2.4 ×10^{25}
4	0.5		0.71		1000±10	2.4 ×10^{25}
5	1.0		0.71		1000±10	4.8 ×10^{25}
6	1.5		0.71		1000±10	7.2 ×10^{25}

Scanning electron microscope (SEM) JSM-6390LV (Jeol, Japan) was used for microstructure characterization. X-ray diffractometer X'PertPRO with Cu Kα radiation was used for X-ray phase analysis. Measurement of the surface profile roughness by Ra parameter was carried out using a profilometer "Proton" model 130 according to GOST 2789-73 at the base length of 0.8 mm.

Hardness determination was carried out using the measuring system FISCHERSCOPE HM2000 S in accordance with the requirements of DIN EN ISO 14577-1. According to the device passport, the hardness measurement range is 0.001-120000 N/mm2, the load setting accuracy is 4 mg, displacements are measured with an accuracy of 0.1 nm. The error of microhardness determination is 2% of the measured value. The indenter feed rate is 2 μm/s. The range of test loads is 0.1-500 mN. A tetrahedral diamond Vickers pyramid with a flat angle of 136° was used as an indenter. The slides for the studies were made according to the standard technique, including mechanical grinding and polishing. Chemical etching in a solution containing 50% hydrofluoric acid and 50% nitric acid was used to reveal the micro-structure of tungsten [13].

3. Results and Discussion

The regimes of irradiation of tungsten with helium ions in the plasma of high-frequency induction discharge leading to the formation of relief structure on the surface of tungsten have been experimentally obtained. The surfaces of the obtained samples were studied on a scanning electron microscope JSM-6390LV. Figure 2 shows the SEM-image of the surface of tungsten samples.

According to the results of microstructural studies of tungsten samples, surface erosion in the form of etched grains and micropores was detected (Figure 2). It was found that in the studied samples microstructure of grains has a different character of changes and has a connection with their crystallographic orientation. While in some grains significant erosion is observed, in other grains the formation of micropores with uneven distribution, which are traces of blister formation, was found. The relief formed consists of chaotically located protrusions and depressions of various shapes. The analysis of experimental results showed that the degree of change in the relief and structure of the surface layer of irradiated samples depends on the type of material and irradiation parameters.

Preprints (www.preprints.org) | NOT PEER-REVIEWED | Posted: 20 November 2023 doi:10.20944/preprints202311.1205.v1

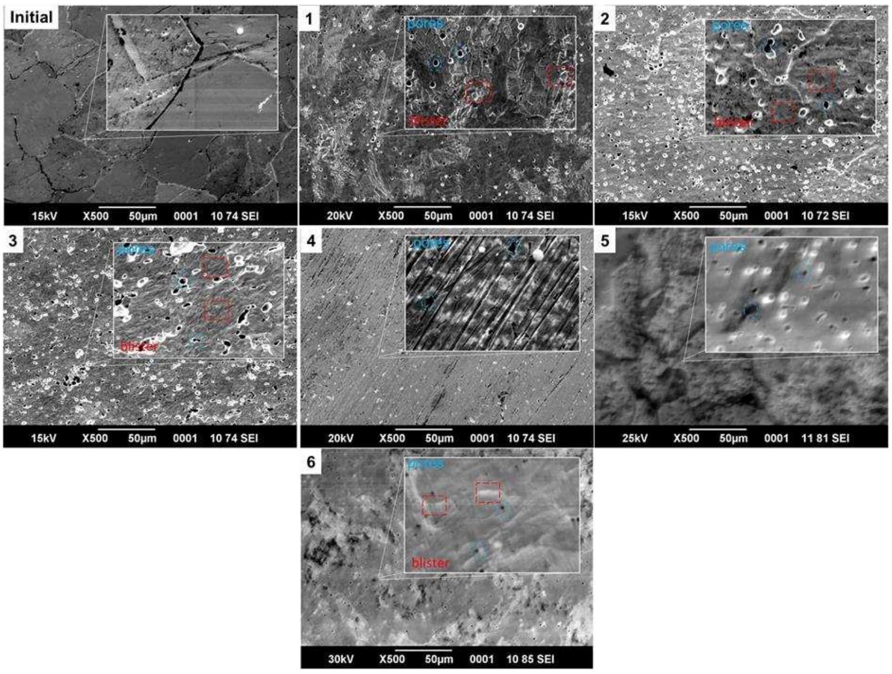

Figure 2. SEM images of the surface of tungsten samples.

The results of the samples on the profilometer are shown in Figure 3. It was determined that after irradiation of tungsten with helium plasma the surface roughness changes depending on the irradiation temperature. The greatest increase in roughness Ra = 0.1406 μm is observed in samples irradiated in regime 5, which is associated with the formation of small protrusions and depressions on the surface layer. At the same time, in the samples irradiated in regime 6, the surface of which is characterized by chaotically located protrusions and depressions of various shapes, the roughness parameter Ra was 0.0603 μm. The smallest change of roughness Ra = 0.0299 μm is observed in the samples irradiated in regime 4. The results obtained are in good agreement with the metallographic analysis. Woller et al. [14] observed that at temperatures lower than that required for fluff formation (from 870 to 1220 K), bundles of nanoenhancers can form on the surface, and this depends on the average ion energy and ion flux density. Therefore, this surface patterning requires further investigation. Thus, it can be stated that during irradiation of tungsten with helium plasma, the main relief forming mechanism is surface sputtering characterized by thermal etching of the surface.

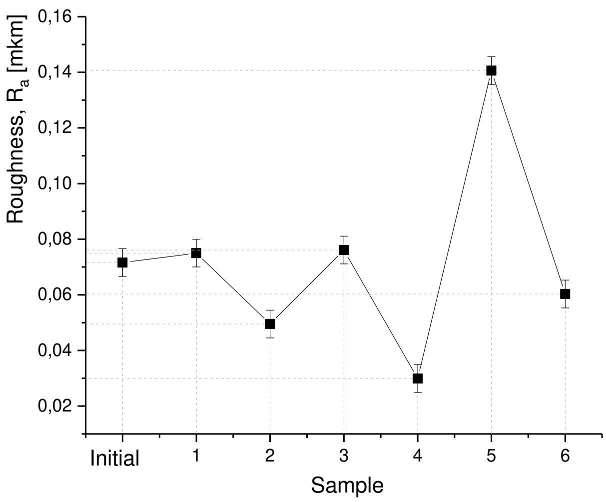

Figure 3. Results of profilometer tests.

The results of diffractograms obtained under different regimes of irradiation of tungsten with helium plasma are shown in Figure 4. When comparing in turn the diffractograms of these samples with each other, an increase in the intensity of peaks is observed.

According to the results of X-ray phase analysis of tungsten samples, we can conclude that the main phase in the samples is the crystalline phase of tungsten with a cubic lattice, space group Im-3m (229). At the same time, the diffractogram of sample 1 shows peaks of low intensity of crystalline phases W as well as a shift of peak (110) towards higher angles, which is caused by the increase of tensile macro-stresses.

Based on the literature data on the radiation resistance of tungsten, we can assume that irradiation creates radiation-induced damage in the lattice of tungsten, namely, displacements of atoms leading to the formation of defects capable of capturing and retaining hydrogen isotopes. Such defects are vacancies and vacancy clusters, as well as dislocation-type defects [15, 16]. In addition, irradiation of tungsten with thermonuclear neutrons leads to transmutation effects, i.e., the appearance of radioactive isotopes of tungsten.

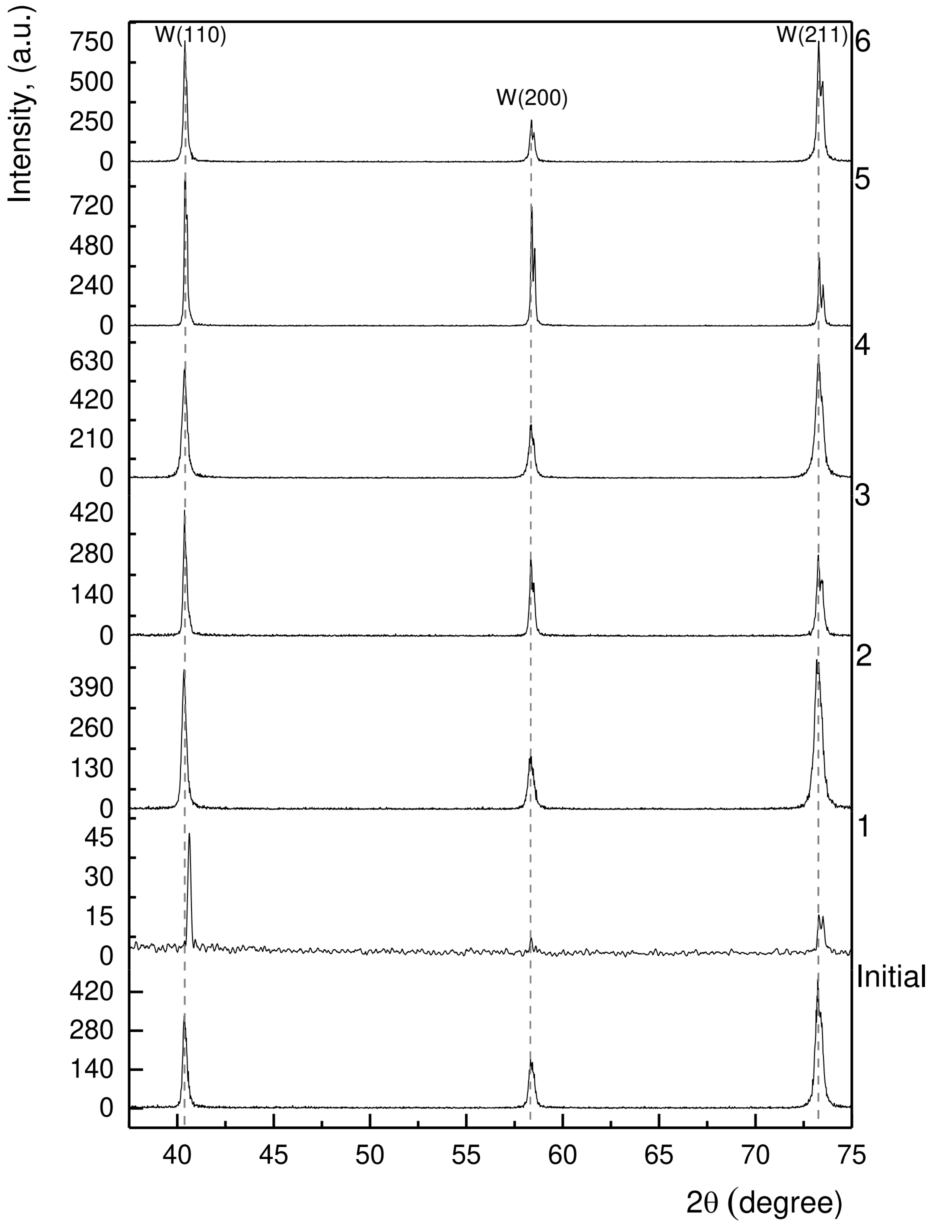

Figure 4. Diffractograms of tungsten before and after helium plasma irradiation at different regimes.

 doi:10.20944/preprints202311.1205.v1

Figure 5 shows the elastic modulus and hardness of the materials irradiated with helium plasma compared to their non-irradiated state, with numerical values given in Table 2. According to Figure 6, the maximum indentation depth is 500 mN. The irradiated sample in regime 1 shows a decrease in hardness to 3182 N/mm2, this value is lower by 31 % compared to the original sample. With increasing target temperature regime of 900°C and 1200°C, the hardness of the samples increases by 5122 N/mm2 and 5081 N/mm2, and the elastic modulus by 419 GPa and 489 GPa, respectively.

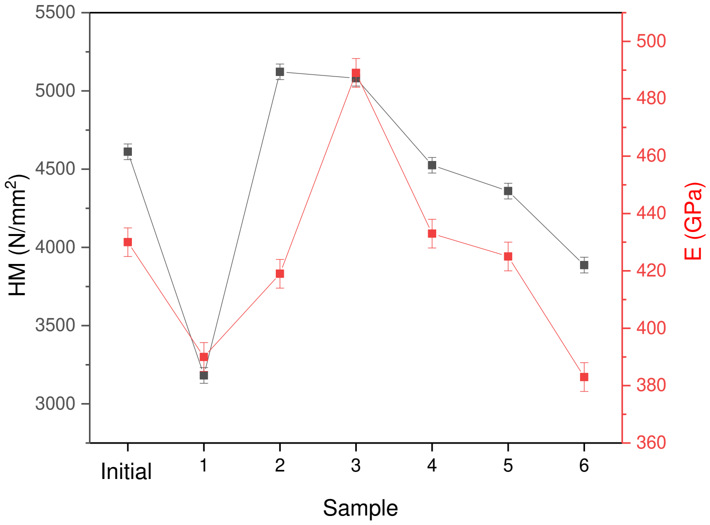

Figure 5. Elastic modulus and hardness of materials irradiated with helium plasma.

Fig. 6 and Table 2 also show that after irradiation there is a noticeable increase in the modulus of elasticity of all samples. As with the increase in hardness, the increase in modulus of elasticity is slightly higher in the irradiated samples than in the original state. In all cases, the increase is perceptible and goes beyond the experimental error limits

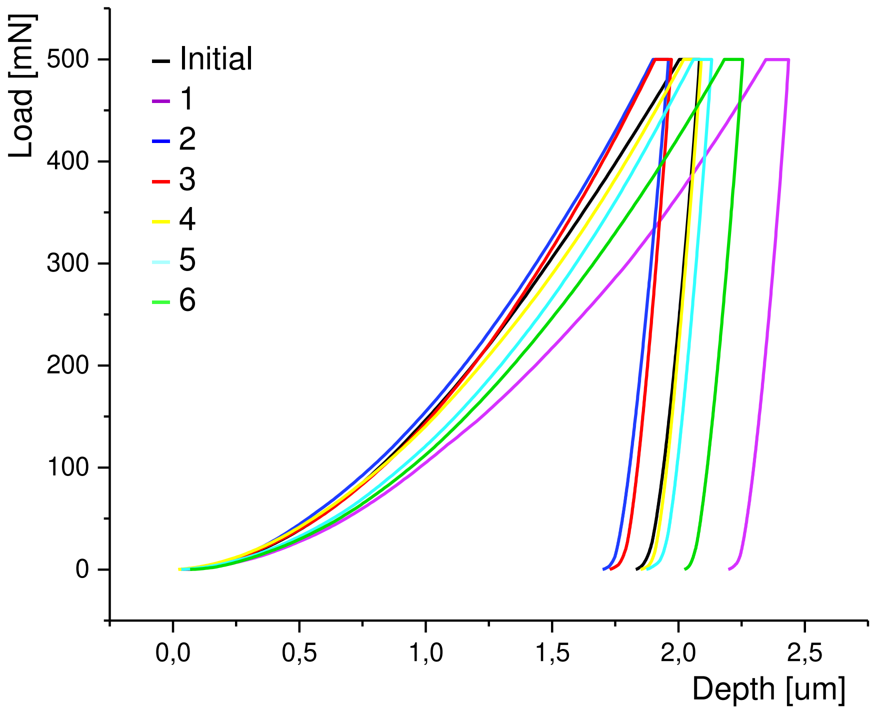

Figure 6. Typical load-displacement curves during indentation.

Table 2. Correlation table of the obtained results.

Sample	Coefficient of friction	HV	HM [N/mm2]	E [GPa]	H/E
Initial	0.744	515	4611	430	10.72326
1	0.648	349	3182	390	8.158974
2	0.683	594	5122	419	12.22434
3	0.616	575	5081	489	10.39059
4	0.654	510	4525	433	10.45035
5	0.648	489	4360	425	10.25882
6	0.101	436	3887	383	10.14883

5. Conclusions

Helium plasma irradiation at different regimes has a strong influence on the structural-phase state and mechanical properties of tungsten. Thus, the following results were obtained:

Plasma irradiation changes the surface topography of tungsten. It is shown that structural changes in the near-surface region of tungsten - pores and blisters - are observed as a result of helium plasma irradiation. X-ray phase analysis showed that no new phases of the W system were found after irradiation, only an increase in the intensity of diffraction lines was observed. There are significant differences in the microstructure of tungsten depending on the temperature of helium plasma irradiation in the above range. It is assumed that the cause of defects is the extremely low solubility of helium in tungsten. At irradiation by plasma as a result of formation of high concentration of helium gas high mechanical stresses arise, initiating surface destruction of the sample and creation of blisters and pores.

It is revealed that after irradiation the surface roughness changes in comparison with the initial sample and no consistent increase or decrease in values according to the treatment regime is observed. It is established that at temperature regimes T = 1200 °C and T = 1500 °C the microhardness of tungsten increases by 11% and 10% respectively.

Prospectivity of application of the simulation stand KAZ-PSI gives the possibility of obtaining the results of experimental studies in a relative but inexpensive way. The obtained data are in demand when designing fusion reactor design elements, analyzing their operating life and the influence of plasma on materials, and predicting the accumulation of isotopes of plasma-forming elements in the fusion reactor volume.

Author Contributions: Z.S. and B.R., A.K. designed the experiments; A.K. and Z.S. performed the experiments; B.R. and Z.S., analyzed the data; Z.S., A.K. and B.R. wrote, reviewed and edited the paper. All authors have read and agreed to the published version of the manuscript.

Funding: This research has been funded by the Science Committee of the Ministry of Science and Higher Education of the Republic of Kazakhstan (Grant no. AP09058568).

Institutional Review Board Statement: Not applicable.

Informed Consent Statement: Not applicable.

Data Availability Statement: Data is contained within the article.

Conflicts of Interest: The authors declare that there is no conflict of interest regarding the publication of this manuscript.

References

1. Miyamoto, M., Mikami, S., Nagashima, H., Iijima, N., Nishijima, D., Doerner, R. P., ... & Sagara, A. Systematic investigation of the formation behavior of helium bubbles in tungsten. *Journal of Nuclear Materials* **2015**, *463, 333-336. https://doi.org/10.1016/j.jnucmat.2014.10.098*
2. Kajita, S., Yoshida, N., Yoshihara, R., Ohno, N., & Yamagiwa, M. TEM observation of the growth process of helium nanobubbles on tungsten: Nanostructure formation mechanism. *Journal of nuclear materials* **2011**, *418(1-3), 152-158. DOI:10.1016/j.jnucmat.2011.06.026*.
3. Nishijima, D., Ye, M. Y., Ohno, N., & Takamura, S. Formation mechanism of bubbles and holes on tungsten surface with low-energy and high-flux helium plasma irradiation in NAGDIS-II. *Journal of nuclear materials* **2004**, *329, 1029-1033. https://doi.org/10.1016/j.jnucmat.2004.04.129*
4. Sagdoldina, Z., Rakhadilov, B., Kurbanbekov, S., Kozhanova, R., & Kengesbekov, A. Effect of irradiation with Si+ ions on phase transformations in Ti–Al system during thermal annealing. *Coatings* **2021**, *11(2), 205. https://doi.org/10.3390/coatings11020205*
5. Rakhadilov, B., Kengesbekov, A., Zhurerova, L., Kozhanova, R., & Sagdoldina, Z. Impact of electronic radiation on the morphology of the fine structure of the surface layer of R6M5 steel. *Machines* **2021**, *9(2), 24.* https://doi.org/10.3390/machines9020024
6. Kögler, R., Anwand, W., Richter, A., Butterling, M., Ou, X., Wagner, A., & Chen, C. L. Nanocavity formation and hardness increase by dual ion beam irradiation of oxide dispersion strengthened FeCrAl alloy. *Journal of Nuclear Materials* **2012**, *427(1-3), 133-139.*
7. Hunn, J. D., Lee, E. H., Byun, T. S., & Mansur, L. K. Helium and hydrogen induced hardening in 316LN stainless steel. Journal of nuclear materials 2000, 282(2-3), 131-136.
8. He, J. C., Tang, G. Y., Hasegawa, A., & Abe, K. Microstructural development and irradiation hardening of W and W–(3–26) wt% Re alloys after high-temperature neutron irradiation to 0.15 dpa. *Nuclear fusion* **2006**, *46(11), 877.*
9. D.E.J. Armstrong, A.J. Wilkinson, S.G. Roberts, Mechanical properties of ion-implanted tungsten5wt% tantalum. *Physica Scripta T145* **2014**, *1–3. DOI 10.1088/0031-8949/2011/T145/014076.*
10. J. Gibson, D. Armstrong, S. Roberts, Òthe micro-mechanical properties of ion irradiated tungsten. *Physica Scripta* **2011**, *159, 1–5. DOI 10.1088/0031-8949/2014/T159/014056.*
11. D.E.J. Armstrong, C.D. Hardie, J.S. Gibson, A.J. Bushby, P.D. Edmondson, S.G. Roberts, Small-scale characterization of irradiated nuclear materials: part II nanoindentation and micro-cantilever testing of ion irradiated nuclear materials, *J. Nucl. Mater* **2015**, *462 (2015) 374–381. DOI: 10.1016/j.jnucmat.2015.01.053.*
12. Rakhadilov, B.; Satbayeva, Z.; Kusainov, A.; Naimankumaruly, E.; Abylkalykova, R.; Sulyubayeva, L. Linear Plasma Device for the Study of Plasma–Surface Interactions. *Appl. Sci.* **2023**, *13, 11673. https://doi.org/10.3390/app132111673.*
13. K.B. Woller, D.G. Whyte, G.M. Wright, Impact of Helium ion energy modulation on tungsten surface morphology and nano-tendril growth. *In: 26th IAEA Fusion Energy Conference* **2016**, *MPT/P5-26.*
14. Barabash, V., Federici, G., Rödig, M., Snead, L. L., & Wu, C. H. Neutron irradiation effects on plasma facing materials. *Journal of Nuclear Materials* **2000**, *283, 138-146. https://doi.org/10.1016/S0022-3115(00)00203-8.*
15. Iida H., Khripunov V., Petrizzi L., Federici G. ITER Nuclear Analysis Report G73 DDD2 W 0.2, 2004.
16. S. Neuville, Quantum electronic mechanisms of atomic rearrangements during growth of hard carbon films, *Surf. Coat. Technol* **2011**. *206, 703–726 https://doi.org/10.1016/j.surfcoat.2011.07.055*